An Underwater Acoustic Localisation System for Assisted Human Diving Operations

Thomas Glotzbach*, Mohammadreza Bayat,**
A. Pedro Aguiar, Antonio Pascoal****

**Ilmenau University of Technology, 98684 Ilmenau,*
Germany (Tel: +49-3677-694107; e-mail: thomas.glotzbach@tu-ilmenau.de).
***Instituto Superior Técnico (IST)/UTL, Laboratory of Robotics and Systems*
in Engineering and Science (LARSyS), Lisbon, Portugal, (e-mail: {mbayat,pedro,antonio}@isr.ist.utl.pt)

Abstract: In this paper we present a solution to the problem of estimating the position and orientation of a moving underwater object using acoustic range measurements relative to moving surface objects that have access to a global navigation system. We start with the description of a standard GPS Intelligent Buoy system (GIB) that employs an Extended Kalman Filter (EKF); then we adapt this principle for the concrete task of tracking a human diver utilizing moving autonomous surface crafts. To this effect, we will introduce an advanced measurement system that improves significantly the estimation quality especially in the described scenario. The paper concludes with a short description of the first sea trials of the new developed system.

Keywords: Underwater navigation, acoustic communication, marine robots, Kalman filtering, diver assistant system.

1. INTRODUCTION

Underwater navigation is a challenging problem. Since global satellite systems like GPS cannot be used, the development of a long-term stable estimation algorithm for position and orientation of an underwater object remains a difficult task. Out of several possibilities, we refer here to the task of estimating the pose of an underwater object by means of acoustic range measurements between the target and a certain number of dynamic surface objects, like buoys or autonomous surface crafts. All units are equipped with acoustic modems to exchange data, which can also be used to measure range among the two units.

To solve the described task, a system that seeks inspiration from the so-called GPS Intelligent Buoy system (GIB) can be used; see e.g. (Alcocer et al., 2007) and (Alcocer, 2009). Fig. 1 depicts the corresponding scenario. In this case, the Reference Objects (ROs) are buoys equipped with GPS. The Target transmits an acoustic ping at fixed time intervals. The ROs measure the times of arrival (TOA). Because the pings are transmitted at predefined planned times, the buoys can compute the travel time of the signal and therefore their distances to the Target. It is important to notice that by the time the acoustic signals emitted by the Target reach the buoys, the Target itself may have changed position. This precluded the use of a simple position algorithm. In these circumstances, an algorithm that embodies in its structure a back and forward propagation strategy must be used. See the next sections for details.

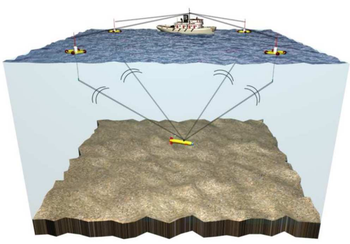

Fig. 1. A standard GIB scenario

Current research tasks aim at the development of assistant systems for human divers (Birk *et al.* 11). In this application, the diver plans a path, which he/she would like to follow in the course of an underwater mission. Special diving equipment is attached to his/her suit, which contains an acoustic communication module, an Inertial Measurement Unit (IMU) and a central processing unit. Stated in simple terms, it is the role of the surface objects to estimate the position of the diver and to issue heading commands to him/her via the acoustic channel so that he/she follows the path with good accuracy. In this scenario, it is the duty of the diver to track the heading commands. This can be done for example by presenting to the diver information about the tracking error and instructing him/her to move left or right, using an array of LEDs installed on the diver´s goggles. In this paper, we focus on the target localization system based on acoustic range measurements. Fig. 2 illustrates the configuration adopted.

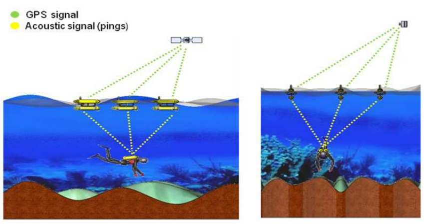

Fig. 2. Scenario for a diver assistant system

The paper is organized as follows. Section 2 describes a general localization problem and introduces some basic notation. Chapter 3 summarizes the set-up adopted to solve the localization problem in the form of an extended Kalman filter. Chapter 4 extends the solution to the diver assistant problem that is the main focus of the paper. Chapter 5 contains the results of practical experiments that validate the solution adopted.

2. GENERAL PROBLEM DESCRIPTION AND BASE NOTATION

We consider a situation where there are a number of *m* surface buoys or Autonomous Surface Crafts, henceforth named as ROs. Using GPS receivers, the ROs can compute their inertial positions with very good accuracy, that is, with errors on the order of centimetres. The ROs are equipped with computational hardware and exchange information via an aerial communication network. Their computer clocks are synchronized via GPS. In addition, each of the ROs is equipped with an acoustic modem capable of receiving acoustic data and computing times of arrival of acoustic signals emitted by a pinger.

In the scenario considered there is also a submerged target, which can be an Autonomous Underwater Vehicle or a human diver. The target moves along a path that is not known in advance. The only a priori knowledge available consists of the maximum linear speed and acceleration, as well as maximum turning rate. The target is equipped with a depth cell. It also carries an acoustic modem, which responds to acoustic pings transmitted in a predefined time interval by one of the ROs and sends the depth information via the acoustic communication link. The key task at hand can be briefly described as follows: compute relevant target motion variables (e.g., position and linear speed) based on measured data that include the target depth and the range between the target and each of the ROs. The following notation will be used: The position of the i^{th} RO at time t_k in the global coordinate system is defined as

$$\mathbf{p_i}(t_k) = [x_i(t_k) \quad y_i(t_k) \quad z_i(t_k)]^T, \tag{1}$$

with $z_i = 0$. In an analogous manner, the target position is given by

$$\mathbf{p}(t_k) = [x(t_k) \quad y(t_k) \quad z(t_k)]^T. \tag{2}$$

3. PROBLEM SOLUTION: THE GENERAL SETUP

3.1 Similarities and differences between the proposed scheme and a GIB-like system

Throughout this paper we will often refer to the model for a standard GIB system introduced in (Alcocer *et* al. 07) and (Alcocer 09). We explore the core ideas exposed in the above references. However, the system that we propose for diver assistance operations or underwater target tracking differs significantly from the basic GIB setup. We start by noticing that the GIB system requires that the clocks on board the ROs and the target be synchronized. A time shift of only one millisecond would create an additional measurement error of about 1.5 meter. It is of course trivial to synchronize the RO clocks, for they maneuver at the surface. Synchronizing the target´s clock is far more difficult and costly. The question then arises as to whether it is possible to develop a GIB-like system that can dispense with the need to synchronize the clocks of all the units involved.

A solution to the above problem requires that the sequence of acoustic emissions aimed at computing ranges (between the target and the ROs) be initiated by one of the ROs, and not by the target itself. This periodically transmitted ping will be referred to as the **reference ping**, while the RO sending it shall be called the **reference**. The target must answer as soon as it receives the reference ping by sending the so-called **target ping**. The time between receiving a reference ping and transmitting a target ping for the target modem is constant and known a priori. The target ping is received by all ROs, the clocks of which are synchronized. Therefore, each RO knows exactly the time at which the reference ping was sent. A measurement model must be developed to capture this set-up in mathematical form. For the time being we shall assume that the target is able to send the target ping immediately after receiving the reference ping, or with a constant time that is known a priori and small in comparison with the runtimes of the pings. We plan to improve this setup to allow for even larger latency times.

3.2 Target Model

For filter design purposes, the kinematic model adopted for the target is a Random Walk with Constant Turning Rate (RWCTR); see (Popaf *et* al., 2004). Because the depth of the target can easily be measured by means of a standard depth cell, the tracking model is considered as a 2D kinematic model. It is straightforward to run a second linear filter for the target depth, which will not be discussed here in detail. The state vector of the target, $\mathbf{x}(t_k)$, consists of five elements: $x(t_k)$ and $y(t_k)$ represent the position of the target, $v(t_k)$ is the magnitude of the linear velocity vector, $\psi(t_k)$ is the angle of the total velocity vector with respect to the x-inertial axis, and $r(t_k)$ represents the rate of change of ψ. Note that $\psi(t_k)$ may be different from the target's heading, as for marine vehicles heading and course angle may differ. In the RWCTR process model the variables v, ψ and r are driven by process noises ξ_v, ξ_ψ, and ξ_r which we assume are stationary, independent, zero-mean, and Gaussian with standard deviations σ_v, σ_ψ, and σ_r respectively. Therefore, the model equations admit the representation

$$\begin{array}{rcl} x(t_{k+1}) & = & x(t_k) + t_{step} \cdot v(t_k) \cdot \cos\psi(t_k) \\ y(t_{k+1}) & = & y(t_k) + t_{step} \cdot v(t_k) \cdot \sin\psi(t_k) \\ v(t_{k+1}) & = & v(t_k) + \xi_v(t_k) \\ \psi(t_{k+1}) & = & \psi(t_k) + t_{step} \cdot r(t_k) + \xi_\psi(t_k) \\ r(t_{k+1}) & = & r(t_k) + \xi_r(t_k) \end{array}, \tag{3}$$

where t_{step} is the step size used in the kinematic model. To separate the process noise from the state transformation matrix, the state model can be written as

$$\mathbf{x}(t_{k+1}) = \overline{\mathbf{A}}(\mathbf{x}(t_k))\mathbf{x}(t_k) + \overline{\mathbf{G}}\xi(t_k) \tag{4}$$

with disturbance vector

$$\xi(t_k) = \left[\xi_v(t_k) \quad \xi_\psi(t_k) \quad \xi_r(t_k)\right]^T$$

and

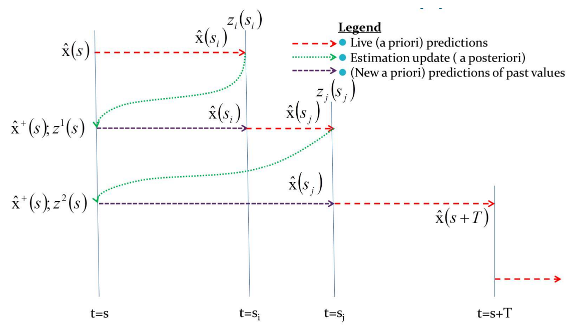

Fig. 3. Back and forward estimation approach

$$\overline{\mathbf{A}}=\begin{bmatrix}1 & 0 & t_{step}\cdot\cos\psi(t_k) & 0 & 0\\ 0 & 1 & t_{step}\cdot\sin\psi(t_k) & 0 & 0\\ 0 & 0 & 1 & 0 & 0\\ 0 & 0 & 0 & 1 & t_{step}\\ 0 & 0 & 0 & 0 & 1\end{bmatrix},\ \overline{\mathbf{G}}=\begin{bmatrix}0&0&0\\0&0&0\\1&0&0\\0&1&0\\0&0&1\end{bmatrix}.$$

3.3 Measurement Model with back and forward approach

We start by describing a generalized model that is key to the Kalman filter design process. We will start with basic concepts and build a model that captures the localization problem at hand. We assume here for the time being that we can obtain noisy range measurements between the target and the i^{th} reference object at time t_k. At this point, we do not dwell into the details of reference and target acoustic pinging.

We start by noticing that whenever the target transmits an acoustic signal (ping) it takes some time until it reaches the ROs and the arrival times are shared via the aerial communication network. This time can be different from one RO to another. During the time, the target may continue to move. Let s be the moment in time when a target ping is sent and s_i the moment when the ping has reached the i^{th} RO. The waiting time due to computation and network transmission time can be dealt with later. At time s_i, we have a measurement of the distance $z_i(s_i)$ between the target position $\mathbf{p}(s)$, and the i^{th} RO position $\mathbf{p_i}(s_i)$. Since we do not have any measurement-based information about the position of the target $\mathbf{p}(s_i)$, a special algorithm is needed to deal with this particular situation. In (Alcocer *et al.* 07) and (Alcocer 09), a back and forward approach is described. Similar concepts were suggested in (Schneider *et al.* 07) and (Schneider *et al.* 08). Fig. 3 captures the basic concepts involved.

After the target sends a ping at time s and the ping is propagating towards the ROs, the centralized computational unit can still only perform a priori predictions using the standard proceedings of a Kalman Filter. At time s_i, the ping is received by i^{th} RO where an a priori estimate $\hat{\mathbf{x}}(s_i)$ is available. Using measurement $z_i(s_i)$, we can compute an a posteriori update for the Kalman Filter, but this needs to be done at time t=s as this is the time when the ping has been sent. As shown in Fig. 3, an a posteriori update is made for the state vector $\mathbf{x}$ at time s, $\hat{\mathbf{x}}^+(s)$, which is assumed to be more precise than the a priori estimation $\hat{\mathbf{x}}(s)$ computed earlier. Then, a new a priori estimate $\hat{\mathbf{x}}(s_i)$ is calculated, which is based on $\hat{\mathbf{x}}^+(s)$. Note that this is again an a priori estimate. The process continues until the target ping is received by other ROs and for each the back and forward algorithm is applied to the states estimate, as Fig. 3 shows. We introduce the vector **z,** which contains the currently available measurements in chronological order:

$$z_i(s_i)=r_i(s_i)+(1+\eta\cdot r_i(s_i))\cdot w_i(s_i) \tag{5}$$

with

$$r_i(s_i)=\|\mathbf{p}(s)-\mathbf{p_i}(s_i)\|=\sqrt{(x(s)-x_i(s_i))^2+(y(s)-y_i(s_i))^2}\ ,$$

where w_i represents measurement noise which is considered to be a Gaussian white noise distribution with zero mean and standard deviation σ'_i. Physical considerations lead us to adopt a model whereby the standard deviation of the measurement noise grows with the distance. Therefore, w_i is multiplied by an expression to bring the range dependency into the equation. η [m^{-1}] expresses the rate of growth of the measurement error with respect to distance. Hence, it can be stated that the true standard deviation can be expressed as:

$$\sigma_i(t_k)=f(d_i(t_k))=(1+\eta\cdot d_i(t_k))\sigma'_i\ , \tag{6}$$

where σ'_i is the base standard deviation for distance equal to zero and d_i is the true distance in 3D at time t_k. We also introduce the diagonal elements of the process noise covariance matrix **Q**, with elements σ^2_v, σ^2_Ψ, σ'_r. Note that equation 5 can also be written in a standard state space form, introducing the system matrices $\overline{\mathbf{C}}$ and $\overline{\mathbf{D}}$, and collecting the measurement and disturbance values in single row vectors **z** and **w** respectively, yielding:

$$\mathbf{z}(t_k)=\overline{\mathbf{C}}(\mathbf{x}(t_k))\mathbf{x}(t_k)+\overline{\mathbf{D}}(\mathbf{x}(t_k))\mathbf{w}(t_k)\,. \tag{7}$$

Similar to equation 7, we introduce the row vector $\hat{\mathbf{z}}(t_k)$ that contains the distances between the estimated position of the target and the true positions of the ROs. The difference between the elements of this vector and those of **z** are needed for the correction step of the Kalman Filter.

3.4 EKF Design for GIB approach

Due to the nonlinear structure of the target model as shown in equations (3) - (7), an Extended Kalman Filter can be used for on-line target tracking. Details on the theory of EKF can be found in [AM 79], [Sim 06], and the references therein.

The key idea behind an EKF is to perform a linearization of the underlying dynamic model about the current estimate. Therefore, the relevant Jacobians have to be computed for the system matrices of equations (3), (4), (5), and (7), yielding:

$$\hat{\mathbf{A}}(\mathrm{x}(t_k))=\left.\frac{\partial f(\mathrm{x},\mathrm{w})}{\partial \mathrm{x}}\right|_{\hat{\mathbf{x}}(t_k)},\ \hat{\mathbf{G}}(x(t_k))=\left.\frac{\partial f(x,w)}{\partial w}\right|_{\hat{\mathbf{x}}(t_k)},$$

$$\hat{\mathbf{C}}_i(\mathrm{x}(t_k))=\left.\frac{\partial \mathbf{r}_i}{\partial \mathrm{x}}\right|_{\hat{\mathbf{x}}(t_k)},\ \hat{\mathbf{D}}_i(\mathrm{x}(t_k))=\left.\frac{\partial \mathbf{z}_i}{\partial \mathrm{w}_i}\right|_{\hat{\mathbf{x}}(t_k)}. \tag{8}$$

The details of the computations of these matrices for the GIB scenario can be found in (Alcocer *et al.* 07). We will show how to compute the $\hat{\mathbf{C}}$ matrix for our advanced measurement model in the diver assistant scenario in the next section.

Using the standard equations for the Extended Kalman Filter, we perform a priori position estimations as long as there are no new measurements available. These result in the a priori state vector estimation, $\hat{\mathbf{x}}(t_{k+1})$, and the uncertainty covariance matrix, $\mathbf{P}(t_{k+1})$. Assuming that at time s_i, a new measurement value is available which is related to the target ping sent at time s, a posteriori updates can be computed for the estimate at time s, again using the standard EKF equations. The results are $\hat{\mathbf{x}}^+(s)$ and $\mathbf{P}^+(s)$. Now, new a priori estimations can be made for $\hat{\mathbf{x}}(t_{k+1})$, either stepwise from s to s_i, or in one step, using the state and covariance transition matrices. Details can be found in (Alcocer *et al.* 07).

4. EXTENSION TO THE DIVER ASSISTANT SYSTEM

4.1. A simple measurement model

For the reference unit, an obvious approach to estimate its distance to the target is to: i) measure the time interval between sending the reference ping and receiving the target ping, ii) compute the overall distance travelled by the acoustic wave by multiplying the abovementioned time interval by the speed of sound, and iii) divide the result by 2. The other ROs can also compute the total distance covered by the reference ping and target ping based on their individual reception times, and subtract the distance between reference and target which can be communicated by the reference via the radio connection.

Note that we have to differentiate between three different times now: i) the time when the reference ping is sent, s_r; ii) the time when the reference ping is received by the target, s_t; iii) the time when the target ping is received by a RO, s_i, s_j, s_k, and so on. For the sake of completeness, we may also introduce a reaction time t_w which is necessary for the target to send the target ping after it has received the reference ping. Although we assumed above that this time is close to zero (and the target movement during this time will be ignored), it may be reasonable to consider it for the calculation of the real runtime of the pings, as even a delay of 1 ms would lead to an additional measurement error of about 1.5 meter.

Note that the times s_r and s_i are known but no information is available about s_t because it is not known when the target sent the target ping. For the approach currently discussed, we assume that the positions of RO and target did not change considerably during the runtime of the two pings. Therefore, by a division by two and considering the reaction time, we can get an estimate $\hat{s}_t$ under the assumption that RO number i is the reference which sent the ping, that is:

$$\hat{s}_t = s_r + \frac{s_i - s_r - t_w}{2} + t_w = \frac{s_i + s_r + t_w}{2}. \tag{9}$$

In order to use the same algorithms as introduced above, we will manipulate the measurement data to simulate the situation when there was no reference ping, but the whole process was initiated by the pings sent by the target in constant time steps. If the modems can measure the exact runtime of both pings (automatically subtracting the waiting time at the target) and if this measurement is stored as $dist_i$ for RO number i that is assumed to be the reference, we obtain that

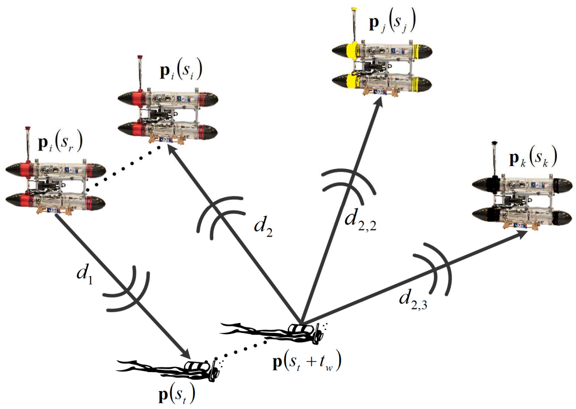

Fig. 4. An illustration of the diver and three MEDUSA autonomous surface vehicles developed at IST.

$$z_i(s_i) = \frac{dist_i}{2}. \tag{10}$$

These values are now used as measurement values for the distance from target at time $\hat{s}_t$ to RO number i at time s_i. For all non-reference ROs (index j), the distances travelled by reference ping and target ping are different. We retrieve the relevant 'measurement data' for the target ping by multiplying the assumed runtime by the speed of sound *v_sound* and subtracting the distance determined for the reference as follows:

$$z_j(s_j) = dist_j - z_i(s_i),\quad z_j(s_j) = (s_j - s_r - t_w)\cdot v\_sound - z_i(s_i) \tag{11}$$

For the EKF, we need the difference between measurement data and the estimated data:

$$\hat{z}_j(s_j) = \sqrt{(\hat{x}(\hat{s}_t) - x_j(s_j))^2 + (\hat{y}(\hat{s}_t) - y_j(s_j))^2}. \tag{12}$$

Finally, the system matrix $\hat{C}$ can be computed as the Jacobian of equation (12) with respect to the elements of $\mathbf{x}(s)$:

$$\hat{\mathbf{C}}_{\mathbf{j}}(s) = \frac{1}{\hat{z}_j(s_j)}\left[(\hat{x}(\hat{s}_t) - x_j(s_j)) \quad (\hat{y}(\hat{s}_t) - y_j(s_j)) \quad 0 \quad 0 \quad 0\right]. \tag{13}$$

The above stated EKF algorithm could in principle be used. We avoided this solution due to two main reasons:

1. In a non-GIB scenario, the ROs will usually not be quasi-stationary buoys and therefore their motion in between pings cannot be ignored. As shown in Fig. 4, the position of the reference when sending the reference ping differs from the one when receiving the target ping. Therefore, there are two different distances d_1 and d_2. It should be possible to consider this fact.

2. In the simplified approach described above, all ROs except the reference require the distance between the reference and the target which is obtained after the reference receives the target ping. At this point is important that the percentage of communication losses can be very high. If the target ping is not received by the reference, the corresponding distance cannot be calculated. As a consequence, even if the other ROs receive the target ping, they will not be able to compute their distances to the target. This is clearly a poor solution to the problem in question, and an obvious waste of communication resources.

4.2 Advanced Measurement Model

We now study a new approach that takes into account the fact that the position of the reference unit when sending the reference ping is different from the one when receiving the target ping. This is shown in Fig. 4. The reference *i* is at position $P_1 = \mathbf{p}_i(s_r)$ when sending the reference ping. The target is at position $P_T = \mathbf{p}(s_t)$ when receiving the reference ping and at $P_T = \mathbf{p}(s_t+t_w)$ when sending the target ping. As discussed before, we will ignore the fact that the target needs some time t_w for answering the ping and that it can also move during this time window, when calculating the positions. Since t_w is assumed to be very small, the movement of the target during t_w can be ignored. Hence, for the measurement of the distance covered by the pings, t_w must be taken into account, due to the relatively high speed of sound. Note also that since we only estimate the time of sending, it is reasonable to treat the problem now as 3D, using the depth of target, $\mathbf{z}(s_t)$, or $\mathbf{z}(s_t+t_w)$, as follows:

$$z_i(s_i) = d_i(s_i) + \left(1+\eta \cdot d_{i,1}(s_t)\right)\cdot w_i(s_t) + \left(1+\eta \cdot d_{i,2}(s_i)\right)\cdot w_i(s_i) \quad (14)$$

with

$$\begin{aligned} d_i(s_i) &= \left\|\mathbf{p}(s_t) - \mathbf{p_i}(s_r)\right\| + \left\|\mathbf{p}(s_t+t_w) - \mathbf{p_i}(s_i)\right\| \\ &= \sqrt{\left(x(s_t) - x_i(s_r)\right)^2 + \left(y(s_t) - y_i(s_r)\right)^2 + z^2(s_t)} \\ &+ \sqrt{\left(x(s_t+t_w) - x_i(s_i)\right)^2 + \left(y(s_t+t_w) - y_i(s_i)\right)^2 + z^2(s_t+t_w)} \end{aligned}.$$

For the computation, we need to estimate the arrival time s_t when we assume that the reference ping is received by the target. We will perform the a posteriori update at that time. In each calculation step the travel distance of the reference ping is calculated (speed of sound times the difference of current time t_k and sending time s_r) and compared with the distance between the reference position when sending the reference ping and the current estimated target position. If the travel distance is greater, we assume that the ping has reached the target at the beginning of the current time step. This assumption will add an error to our estimation, which can be disregarded. As an example, if the target moves with 0.5 m/s, for simulation purposes, time steps of 10 ms can be used, so the error cannot exceed $5*10^{-3}$ m. In reality, when bigger time steps are available, like 0.1 s, still the maximum error is at $5*10^{-2}$ m which is below the measurement errors of the ranging devices.

Therefore, we can state that the estimated measurement distance is given by (using the estimated target depth $\hat{z}(s_t)$ or $\hat{z}(s_t+t_w)$ from the mentioned second filter system)

$$\begin{aligned} \hat{z}_i(s_i) = \hat{d}_1 + \hat{d}_2 &= \sqrt{\left(\hat{x}(\hat{s}_t) - x_i(s_r)\right)^2 + \left(\hat{y}(\hat{s}_t) - y_i(s_r)\right)^2 + \hat{z}^2(s_t)} \quad (15) \\ &+ \sqrt{\left(\hat{x}(\hat{s}_t+t_w) - x_i(s_i)\right)^2 + \left(\hat{y}(\hat{s}_t+t_w) - y_i(s_i)\right)^2 + \hat{z}^2(s_t+t_w)} \end{aligned}$$

The elements of the system matrix $\hat{\mathbf{C}}$ can be computed as

$$\hat{\mathbf{C}}_j(s) = \begin{bmatrix} \dfrac{\hat{x}(\hat{s}_t) - x_i(s_r)}{\hat{d}_1} + \dfrac{\hat{x}(\hat{s}_t+t_w) - x_j(s_j)}{\hat{d}_2} \\ \dfrac{\hat{y}(\hat{s}_t) - y_i(s_r)}{\hat{d}_1} + \dfrac{\hat{y}(\hat{s}_t+t_w) - y_j(s_j)}{\hat{d}_2} \\ [0 \quad 0 \quad 0]^T \end{bmatrix}^T \quad (16)$$

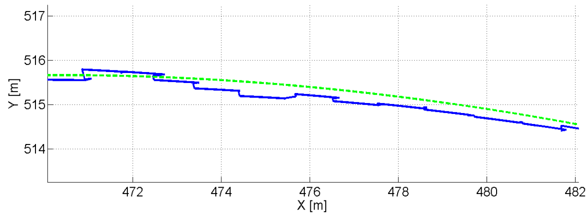

Fig. 5. Simulation in MATLAB®

As explained before, there is a small inaccuracy in this solution, because for the first square root we computed the gradient with respect to $\hat{x}(s_t)$, while for the second one it was computed with respect to $\hat{x}(s_t+t_w)$. Future investigation will deal with the exact formulation and the comparison of the results. With this set-up, an EKF approach can now be used. Note that according to equation (16), the measurement of RO number *j* can be used even if no measurement from the reference *i* is available, as the information for s_i or $p_i(s_i)$ is not needed for the calculation of $\hat{\mathbf{C}}_j$.

5. VALIDATION

5.1. Simulations

The algorithm was validated in simulation using MATLAB®. Table 1 shows the results of 6 simulations; the details are described below. For each simulation, the mean and variance of the absolute 2D estimation error is expressed in meters. The first two values are for the a priori estimates (each time step), the second pair is from all a posteriori estimates whenever a new measurement was available.

Table 1: Results of MATLAB®-simulations

	Absolute Error [m]	Simulation Number						
		1	2	3	4	5	6	Mean
A priori estimate	Mean	0.29	0.32	0.34	0.30	0.34	0.32	0.32
	Variance	0.03	0.04	0.04	0.02	0.03	0.02	0.03
A posteriori estimate	Mean	0.28	0.31	0.33	0.29	0.32	0.30	0.31
	Variance	0.03	0.04	0.04	0.03	0.03	0.03	0.03

Base data: Step size 0.01 s. Target moved on an ellipse: Center 500 m, 450 m; Length of diagonals 80m, 50m; Angle of Orientation -0.75; Target velocity: 0.2 m/s. Target depth: z(t) = 50 [m] - 50 [m] * cos(0.02 [1/s] * t). 3 ROs placed at (300,300,0); (700,300,0); (500,700,0) [m], moving with RWCA, acceleration variance 0.1 m^2/s^4, maximum velocity 1 m/s, within 75 m around initial positions. Modems interrogation frequency 0.2 [Hz]. Target reaction time 1 s. Range and depth measurements disturbed by white noise: mean value = 0 m; variance = 0.1 m^2, η= 0.001. Initial Values for EKF: Q = [1e-8 0 0;0 2.5e-12 0;0 0 4e-11]; P = [400 0 0 0 0;0 400 0 0 0;0 0 0.25 0 0;0 0 0 0.0025 0;0 0 0 0 2.5e-005]. A time of 33 minutes, and 20 seconds has been simulated in 200,000 steps.

Fig. 5 shows part of the target trajectory as a dash line, together with the a priori estimations by the tracking system as a solid line. The jumps result from the a posteriori estimations after new measurements become available.

5.2. Sea Trials

The method proposed was tested extensively in many trials. An example of one of the trials is shown in figures 6 and 7, that display the trajectories of 3 autonomous surface vehicles called MEDUSAs in an assistant mission scenario where the diver is required to follow a predefined U path. In this scenario a pole carried by the diver underwater is fixed to a buoy carrying a GPS at the surface. The modem is attached to the other end of the pole, which is 2 meters deep in the water. Guidance commands are sent through the acoustic channel to the modem of the diver, which are then translated into LED lights on the Goggles to guide the diver. The GPS signal is used only for ground-truthing. The whole formation is moving with a nominal speed of about 0.4 [m/s], while the modems are operated at a frequency of 0.2 [Hz]. In each interrogation the reference sends the reference commands to the diver, and the diver in response sends back its depth and heading. Figures 6 and 7 show the results of the mentioned U mission, which was done in real time. The original RTK-GPS positions of the Medusas that play the roles of ROs are shown in dash lines. The location of the diver who is carrying the surface buoy with a GPS receiver is shown as a solid line. The online estimated location of the diver is shown by the piecewise continuous dotted curve. Figure 8 shows the estimation error as a function of mission time.

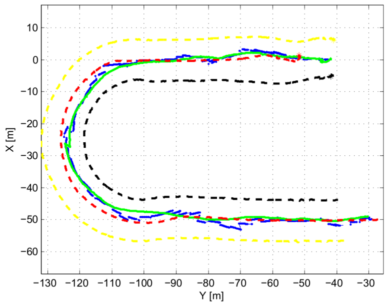

Fig. 6. Results from Sea Trials: MEDUSA paths (dash lines) and diver path (solid line)

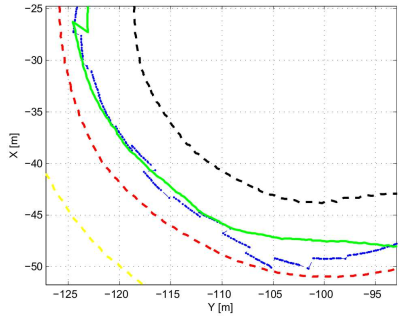

Fig. 7. Results from Sea Trials (Zoom)

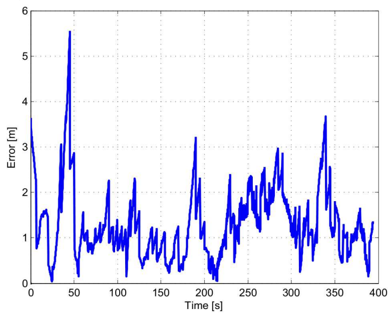

Fig. 8. Estimation Error (Distance between estimated and measured position)

6. CONCLUSIONS

The paper described the design, implementation, and actual testing of an EKF-based underwater target positioning system for assisted diving operations. At the core of the system developed is a GIB-like structure, whereby the position of an underwater target is estimated by measuring the ranges between the diver and a set of moving autonomous surface vehicles equipped with acoustic modems that also work as ranging devices. Unlike the pure GIB approach, the new system does not require that the clocks of the surface units and the underwater target be synchronized. Furthermore, the set-up adopted yields robustness against brief acoustic signal losses. The results obtained in simulation and during tests with a human diver show that the system developed holds good potential for practical applications in assisted diver or AUV operations. Future work will address the extension of the techniques developed to deal with more than one target simultaneously and with scenarios in which the reference objects are also underwater systems.

ACKNOWLEDGMENTS

This research was supported in part by the Marie Curie Intra European Fellowship ‘CONMAR’ (N° 255216) and the Collaborative Project ‘MORPH’ (N° 288704), both founded by the 7th European Community Framework Programme, and by project CONAV/FCT-PT [PTDC/EEACRO/ 113820/2009]. The second author benefited from a PhD scholarship of the Foundation for Science and Technology (FCT), Portugal.

REFERENCES

Alcocer, A., Oliveira, P., Pascoal, A. (2007). Study and implementation of an EKF GIB-based underwater positioning system. In *Control Engineering Practice*, Volume 15, Issue 6, June 2007, Pages 689–701.

Alcocer, A. (2009) Positioning and Navigation Systems for Robotic Underwater Vehicles. *PhD Dissertation thesis* of the Instituto Superior Técnico, Lisbon, October 2009.

Anderson, B. D. O., Moore, J. B. (1979). *Optimal filtering*. Englewood Cliffs, NJ: Prentice-Hall.

Popaf, D., Sandersont, A., Komerskat, R., Mupparapd, S., Blidberg, D., and Chappelf, S. (2004) Adaptive sampling algorithms for multiple autonomous underwater vehicles. In Proc. *IEEE /OES Autonomous Underwater Vehicles* AUV ’04, 2004.

Schneider, M., Glotzbach, T., Jacobi, M., Müller, F., and Otto, P. (2007) Observer-Based Position Estimation for Coordinated Motion Control of Multiple Unmanned Marine Vehicles. In Proc. of *The 17th International Offshore (Ocean) and Polar Enigneering Conference & Exihibition*, ISOPE, 2007, Lisbon, Portugal, CD-ROM-Proceedings, pp. 1059-1065.

Schneider, M., Glotzbach, T., Jacobi, M., Müller, F., Eichhorn, M., and Otto, P. (2008) Kalman filter based team navigation for Multiple Unmanned Marine Vehicles. In Proc. *IEEE International Conference on Control Applications* (CCA 2008), 2008, San Antonio, USA, Conference CD-ROM Proceedings, pp. 565-570.

Simon, D. (2006) *Optimal State Estimation*, John Wiley & Sons, 2006.

Birk, A., Antonelli, G., Caiti, A., Casalino, G., Indiveri, G., Pascoal, A., Caffaz, A. (2011) The CO3AUVs (Cooperative Cognitive Control for Autonomous Underwater Vehicles) project: Overview and current progresses. In Proc of *IEEE OCEANS*, 2011 - Spain, pp.1-10, 6-9 June 2011.